Cancer Research

CCR5$^+$ Myeloid-Derived Suppressor Cells Are Enriched and Activated in Melanoma Lesions

Carolin Blattner[1,2], Viktor Fleming[1,2], Rebekka Weber[1,2], Bianca Himmelhan[1,2], Peter Altevogt[1,2], Christoffer Gebhardt[1,2], Torsten J. Schulze[3], Hila Razon[4], Elias Hawila[4], Gizi Wildbaum[4], Jochen Utikal[1,2], Nathan Karin[4], and Viktor Umansky[1,2]

Abstract

Accumulation of myeloid-derived suppressor cells (MDSC) in melanoma microenvironment is supported by chemokine receptor/chemokine signaling. Although different chemokines were suggested to be involved in this process, the role of CCR5 and its ligands is not established. Using a *Ret* transgenic mouse melanoma model, we found an accumulation of CCR5$^+$ MDSCs in melanoma lesions associated with both increased concentrations of CCR5 ligands and tumor progression. Tumor-infiltrating CCR5$^+$ MDSCs displayed higher immunosuppressive activity than their CCR5$^-$ counterparts. Upregulation of CCR5 expression on CD11b$^+$Gr1$^+$ myeloid cells was induced *in vitro* by CCR5 ligands and other inflammatory factors. In melanoma patients, CCR5$^+$ MDSCs were enriched at the tumor site and correlated with enhanced production of CCR5 ligands. Moreover, they exhibited a stronger immunosuppressive pattern compared with CCR5$^-$ MDSCs. Blocking CCR5/CCR5 ligand interactions increased survival of tumor-bearing mice and was associated with reduced migration and immunosuppressive potential of MDSCs in tumor lesions. Our findings define a critical role for CCR5 in recruitment and activation of MDSCs, suggesting a novel strategy for melanoma treatment.

Significance: These findings validate the importance of the CCR5/CCR5 ligand axis not only for MDSC recruitment but also for further activation of their immunosuppressive functions in the tumor microenvironment, with potentially broad therapeutic implications, given existing clinically available inhibitors of this axis. *Cancer Res; 78(1); 157–67. ©2017 AACR.*

Introduction

A strong immunosuppressive network is typical for melanoma microenvironment, where a heterogeneous population of myeloid-derived suppressor cells (MDSC) plays a major role (1–4). These cells express CD11b and Gr1 in tumor-bearing mice and contain monocytic (M) and polymorphonuclear (PMN) subsets (5). In cancer patients, M-MDSCs are defined as Lin$^-$HLA-DR$^{-/low}$CD11b$^+$CD14$^+$CD15$^-$ and PMN-MDSCs as Lin$^-$HLA-DR$^{-/low}$CD11b$^+$CD14$^-$CD15$^+$CD33$^+$ cells (6–8). MDSCs can inhibit the antitumor reactivity of T and NK cells via different mechanisms, including the production of reactive oxygen species (ROS) and nitric oxide (NO) as well as the expression of programmed death-ligand 1 (PD-L1) and arginase (ARG)-1 (1–3, 6–9). A long-term secretion of various inflammatory factors by tumor and stroma cells promotes generation, recruitment, and activation of MDSCs in tumor lesions (4, 9–11).

Chemokines are known to regulate the trafficking of lymphocytes and myeloid cells through interactions with specific transmembrane, G protein–coupled C– chemokine receptors (CCR; ref. 12). The CCR5 is a key CCR that binds three chemokines: CCL3 (MIP-1α), CCL4 (MIP-1β), and CCL5 (RANTES; ref. 13). It was found that males bearing a functional mutation in CCR5 (delta 32) acquired resistance to the development of prostate cancer (14). Furthermore, the expression of CCR5 ligand CCL5 correlated with breast cancer progression (15) and enhanced melanoma growth in nude mice (16). The treatment with CCL5 antagonist suppressed tumor growth in a breast cancer model (17). Moreover, CCR5 inhibitors were demonstrated to inhibit growth and metastasis of pancreatic (18), prostate (19), and breast tumors (20). In colorectal cancer patients with liver metastases, the CCR5 blockade by maraviroc induced the repolarization of tumor-associated macrophages and resulted in beneficial clinical responses (21).

The importance of chemokine CCL2 and its receptors in the attraction of M-MDSCs was well described (22–24). However, the role of CCR5 and its ligands in MDSC mobilization and activation in melanoma microenvironment is poorly understood. In this study, we addressed this question in a *Ret* transgenic mouse melanoma model that closely resembles human melanoma (25, 26) as well as in melanoma patients at different stages. We found an accumulation of CCR5$^+$ MDSCs in melanoma lesions that was associated with increased production of CCR5 ligands at the tumor site. Importantly, CCR5$^+$ MDSCs displayed stronger immunosuppressive pattern and function in tumor-bearing mice and melanoma patients than their CCR5$^-$ counterparts. Fusion protein mCCR5–Ig-neutralizing CCR5 ligands,

[1]Skin Cancer Unit, German Cancer Research Center (DKFZ), University Medical Center Mannheim, Ruprecht-Karl University of Heidelberg, Heidelberg, Germany. [2]Department of Dermatology, Venereology, and Allergology, University Medical Center Mannheim, Ruprecht-Karl University of Heidelberg, Mannheim, Germany. [3]Institute of Transfusion Medicine and Immunology, Medical Faculty Mannheim, Heidelberg University, German Red Cross Blood Service Baden Württemberg-Hessen, Mannheim, Germany. [4]Department of Immunology, Faculty of Medicine, Technion-Institute of Technology, Haifa, Israel.

Note: Supplementary data for this article are available at Cancer Research Online (http://cancerres.aacrjournals.org/).

C. Blattner and V. Fleming share first authorship of this article.

N. Karin and V. Umansky share senior authorship of this article.

Corresponding Authors: Viktor Umansky, German Cancer Research Center (DKFZ), University Medical Center Mannheim, Im Neuenheimer Feld 280, Heidelberg 69120, Germany. Phone: 4962-1383-3773; Fax: 4962-1383-2113; E-mail: v.umansky@dkfz.de; and Nathan Karin, Technion-Institute of Technology, Haifa, Israel. E-mail: nkarin10@gmail.com

doi: 10.1158/0008-5472.CAN-17-0348

reduced migration, and immunosuppressive potential of MDSCs in the tumor microenvironment and significantly improved survival of tumor-bearing mice.

Materials and Methods

Mice

Mice (C57BL/6 background) expressing the human *Ret* transgene in melanocytes under the control of mouse metallothionein-I promotor-enhancer (25) were provided by Dr. I. Nakashima (Chubu University, Aichi, Japan). Healthy C57BL/6 mice (6–8 weeks) were purchased from Charles River Laboratories. Mice were kept under pathogen-free conditions in the animal facility of German Cancer Research Center (Heidelberg, Germany). Animal studies have been conducted in accordance with an Institutional Animal Care and Use Committee (IACUC).

Patients

Peripheral blood and metastases were obtained from 66 melanoma patients of stage I–IV (AJCC 2009) who were seen at the Skin Cancer Center (University Medical Center Mannheim, Germany) from January 2013 to August 2015. The patient studies were conducted in accordance with the Declaration of Helsinki and approved by the local Ethics Committee (2010-318N-MA). The group contained 47 males (71.2%) and 19 females (28.8%) with the mean age of 62.37 years (range, 33–90 years); 16 patients had stage I (24.2%), 20 patients had stage II (30.3%), 19 patients had stage III (28.8%), and 11 patients had stage IV (16.6%). Patients were not treated within the last 6 months before blood sampling. Peripheral blood from 14 age- and gender-matched healthy donors (HD) without indications of immune-related diseases were obtained at the Institute of Transfusion Medicine and Immunology, Medical Faculty Mannheim, Heidelberg University, German Red Cross Blood Service Baden Württemberg–Hessen (Mannheim, Germany) after informed consent.

Reagents and antibodies

mCCR5–Ig was constructed as previously described (27) and provided by *InVivo* BioTech Services. Control anti-mouse IgG was from Sigma-Aldrich. CCL3, CCL4, CCL5, GM-SCF, IL6, IL10, IFNγ and IL1β were purchased from PeproTech. Anti-mouse monoclonal antibodies (mAb) CD11b-APC-Cy7, Gr1-PE-Cy7, Ly6C-FITC; Ly6C-APC, CD195-PE, PD-L1-APC, CD45.2-PerCP-Cy5.5, CD3-PerCP-Cy5.5, CD4-PE-Cy7, CD25-APC, CD279-PE, CD279-BV421, CD69-APC were provided by BD Biosciences; CD8-eFluor450, Foxp3-FITC and Foxp3 fixation/permeabilization kit were from eBioscience, CCR5 (CD195)-APC, CD195-AlexaFluor-488 and CD25-APC-Cy7 were provided by Biolegend. Anti-human mAbs CD11b-APC, HLD-DR-APC-H7, CD14-PerCP, CD15-PE, PD-L1-PE-Cy7, CD4-PE-Cy7, CD4-APC-C7, CD8-APC-Cy7, CD25-PE, CD274-PE, and CD195-BV421 were from BD Biosciences; CD127-FITC, FoxP3-FITC, FoxP3-APC, CD45RA-PE-Cy7; CD3-PerCP-Cy5.5, CD45-PerCP, CD247-FITC, carboxyfluorescein succinimidyl ester (CFSE) and RBC Lysis Buffer were provided by Biolegend. Anti-human ARG-1 mAbs cross-reacting to mouse ARG-1 were from R&D Systems. FcR-Blocking Reagent, MDSC Isolation Kit and $CD8^+$ T-cell Isolation Kit were from Miltenyi Biotech. Intracellular NO and ROS were detected using the respective kits (both from Cell Signaling Technology) according to the manufacturer's instructions.

Treatment with mCCR5–Ig

Ret transgenic tumor-bearing mice were injected intraperitoneally with 10 mg/kg mCCR5–Ig in 0.3 mL PBS twice/week during 4 weeks. The control group of mice with tumors of similar size received 10 mg/kg of control IgG in 0.3 mL PBS with the same intervals. Both groups were monitored daily for tumor progression.

Preparation of cell suspensions

Fresh bone marrow, spleen, lymph node (LN), and tumor samples from transgenic mice were mechanically dissociated in ice-cold PBS and filtered through the cell strainers (BD Falcon). Tumor, bone marrow, spleen, and peripheral blood samples were depleted of erythrocytes by RBC Lysis Buffer and washed twice. Heparinized blood samples from melanoma patients and HDs were subjected to the density gradient centrifugation using Biocoll (Biochrom). Isolated peripheral blood mononuclear cells (PBMC) were cryopreserved in X-VIVO medium (Lonza) supplemented with 30% human serum and 10% DMSO in liquid nitrogen.

Serum collection

Mouse and human peripheral blood samples were centrifuged at 3,000 rpm for 10 minutes. Serum was collected, aliquoted, and stored at −80°C.

Culture of $CD11b^+Gr1^+$ cells *in vitro*

$CD11b^+Gr1^+$ cells were isolated from the bone marrow of healthy C57BL/6 mice using the MDSC Isolation Kit with the purity of around 90%. In various experiments, 10^6 cells were incubated with IL6 (40 ng/mL) or combination of IL6 and GM-CSF (40 ng/mL) or with mixture of IL6, IL10 (5 ng/mL) and GM-CSF (Mix 1), mixture of CCL3 (10 ng/mL), CCL4 (15 ng/mL), CCL5 (50 ng/mL), IL6 and GM-CSF (Mix 2) or combination of CCL3, CCL4, CCL5, IFNγ (2 ng/mL), IL1β (5 ng/mL), IL6, IL10, and GM-CSF (Mix 3) for 2 hours at 37°C. The expression of CCR5, PD-L1, and ARG-1 was measured by flow cytometry.

Flow cytometry

Cells were treated with FcR-blocking reagent and stained with mAbs for 30 minutes at 4°C. For FoxP3 and ARG-1 stainings, samples were preincubated for 45 minutes at 4°C with FoxP3 fixation/permeabilization kit. Acquisition was performed by six- or seven-color flow cytometry using FACSCanto II with FACSDiva 6.0 software (BD Biosciences). Dead cell exclusion was based on the scatter profile. The compensation was performed with BD CompBeads set (BD Biosciences) using the manufacturer's instructions. FlowJo software (Tree Star) was used to analyze at least 500,000 events.

In vitro proliferation assay

Single tumor-cell suspension obtained at room temperature was subjected to density gradient centrifugation using Histopaque 1119 (Sigma-Aldrich). $CCR5^+$ and $CCR5^-$ MDSCs were sorted from isolated tumor-infiltrating leukocytes by FACSAria cell sorter (BD Biosciences). The purity of sorted cell populations was >90%. $CD8^+$ T cells were isolated from spleens of healthy mice using the naïve $CD8^+$ T-cell Isolation Kit (Miltenyi Biotec) according to the manufacturer's instructions and labeled with 1 μM CFSE. T cells were stimulated with anti-CD3/CD28 Dynabeads (Thermo Fisher Scientific) and cocultured with sorted $CCR5^+$ or $CCR5^-$ MDSCs at

the indicated ratio for 72 hours. T-cell proliferation was evaluated by CFSE dilution by flow cytometry.

In vitro cell migration assay

Migration of CD11b$^+$Gr1$^+$ immature myeloid cells was evaluated using a Transwell system as previously described (28) with some modifications. Briefly, upon isolation of CD11b$^+$Gr1$^+$ cells from the bone marrow of C57BL/6 mice using MDSC isolation kit, 2×10^6 cells were incubated for 3 hours at 37°C in medium supplemented with GM-CSF (40 ng/mL) and IL6 (40 ng/mL) in the upper chamber of a polycarbonate Transwell culture insert (Costar). The lower chamber contained CCL3 (10 ng/mL), CCL4 (15 ng/mL), CCL5 (50 ng/mL), and mCCR5–Ig fusion protein (20 ng/mL) or anti-mouse IgG (20 ng/mL). The transmigrated cells in the lower chamber were collected and counted.

Bio-Plex assay

Frozen mouse and human tumor samples were mechanically disrupted and treated with lysis solution (Bio-Rad). After sonication, samples were centrifuged at 4,500 × *g* for 20 minutes at 4°C. Protein amounts were determined using the Pierce BCA Protein Assay Kit (Thermo Fisher Scientific). Concentrations of CCR5 ligands and other factors in samples were measured by multiplex technology (Bio-Rad) according to the manufacturer's instruction. Acquisition and data analysis were performed by Bioplex Manager.

Immunofluorescence

Consecutive cryostat sections of tumors from *Ret* transgenic mice (10 μm in thickness) were fixed in 4% paraformaldehyde overnight, washed, and blocked with PBS containing 1% BSA, 0.1% Triton and 0.2% Fish skin gelatin (Sigma-Aldrich) for 1 hour at room temperature. Sections were stained with CD195-AlexaFluor-488 mAbs as well as primary rabbit anti-mouse Gr1 (Abcam) and rat anti-mouse CD11b (BD Biosciences) mAbs followed by secondary goat anti-rabbit AlexaFluor-568 (Invitrogen) and goat anti-rat AlexaFluor-647 (both Invitrogen) mAbs. Slides were mounted with Roti-Mount FluorCare medium (Roth), and immunofluorescence was detected using confocal microscope (Leica).

Statistical analysis

Statistical analyses were performed using GraphPad Prism software. Data were analyzed with a one-way ANOVA test for multiple groups or an unpaired two-tailed Student *t* test for two groups. A value of $P < 0.05$ was considered as statistically significant.

Results

CCR5$^+$ MDSCs accumulate in melanoma lesions of transgenic mice during tumor progression

We analyzed CCR5$^+$ MDSCs in primary tumors, metastatic LN, bone marrow, peripheral blood, and spleen from *Ret* transgenic mice at different steps of tumor development (Fig. 1). Using immunofluorescence, we found that CD11b$^+$Gr1$^+$CCR5$^+$ MDSCs infiltrated skin tumors (Fig. 1A). The frequency of CCR5-expressing MDSCs in melanoma lesions (skin tumors and metastatic LN) measured by flow cytometry was elevated compared with that in the bone marrow and peripheral blood (Fig. 1B and C; $P < 0.001$). An accumulation of CCR5$^+$ MDSCs in primary tumors (Fig. 1D; $P < 0.01$) significantly correlated with the increasing weight of these tumors. The level of CCR5 expression on MDSCs in melanoma lesions measured by mean fluorescence intensity (MFI) was also upregulated during tumor progression (Fig. 1E; $P < 0.01$).

Comparing the expression of CCR5 on both MDSC subsets, we found a significantly higher frequency of CCR5$^+$ cells among CD11b$^+$Ly6G$^+$Ly6C^{low} PMN-MDSCs in metastatic LN and spleen than among M-MDSCs (Fig. 1F; $P < 0.001$). These findings suggest that CCR5 could serve as a driver for the migration of MDSCs to melanoma lesions.

CCR5 ligands induce trafficking of CCR5-expressing myeloid cells

To study the mechanism of CCR5$^+$ MDSCs recruitment to the tumor site, we measured the production of CCR5 ligands CCL3, CCL4, and CCL5 in serum and melanoma lesions using the same mice as above. The concentration of all three ligands in lysates of skin melanomas and metastatic LN was significantly higher than in serum (Supplementary Fig. S1A–S1C; $P < 0.001$). Furthermore, an accumulation of CCL3 and CCL5 in the tumor microenvironment correlated with the progression of melanoma (Supplementary Fig. S1D and S1E). These results indicate that the secretion of CCR5 ligands could support the accumulation of CCR5$^+$ MDSCs in melanoma microenvironment. To evaluate a direct effect of CCR5 ligand, we measured the migration of bone marrow–derived CD11b$^+$Gr1$^+$ immature myeloid cells (IMC) *in vitro* in the Transwell assay. IMC migration was stimulated by chemokine treatment as compared with unstimulated cells, whereas the fusion protein mCCR5–Ig, neutralizing CCR5 ligands, blocked this effect completely (Supplementary Fig. S1F; $P < 0.05$).

CCR5$^+$ MDSCs display stronger immunosuppressive phenotype and function

We next investigated the key factors involved in the induction of MDSC-mediated immunosuppression like NO, ROS, PD-L1, and ARG-1 (1, 5). Interestingly, the frequency of ARG-1$^+$ cells within CCR5$^+$ MDSCs in melanoma lesions, the peripheral blood and spleen was significantly higher than in their CCR5$^-$ counterparts (Fig. 2A; $P < 0.05$). The intensity of ARG-1 expression in these cells was also strongly increased (Supplementary Fig. S2A; $P < 0.05$). Furthermore, CCR5$^+$ MDSCs displayed a profound elevation of ROS production as compared with CCR5$^-$ cells (Fig. 2B; $P < 0.05$). Melanoma progression in transgenic mice was associated with increased ARG-1 expression and ROS production in CCR5$^+$ MDSCs from skin tumors (Fig. 2C and D; $P < 0.03$) and metastatic LN (Supplementary Fig. S2B and C; $P < 0.02$). Investigating other immunosuppressive factors, we demonstrated a similar elevation of PD-L1 expression and NO production in CCR5$^+$ MDSCs as compared with their CCR5$^-$ counterparts (Supplementary Fig. S2D and S2E; $P < 0.05$). The upregulation of PD-L1 expression in CCR5$^+$ MDSC-infiltrating primary tumors (Supplementary Fig. S2F; $P < 0.04$) was also found to correlate with melanoma progression in these mice.

Next, we verified an immunosuppressive activity of CCR5$^+$ MDSCs using an inhibition of T-cell proliferation assay. Upon isolation from the skin tumors of melanoma-bearing mice by the gradient centrifugation and FACS sorting, CCR5$^+$ MDSCs and CCR5$^-$ MDSCs were cocultured with CFSE-labeled stimulated purified CD8$^+$ T cells. We demonstrated that CCR5$^+$ MDSCs

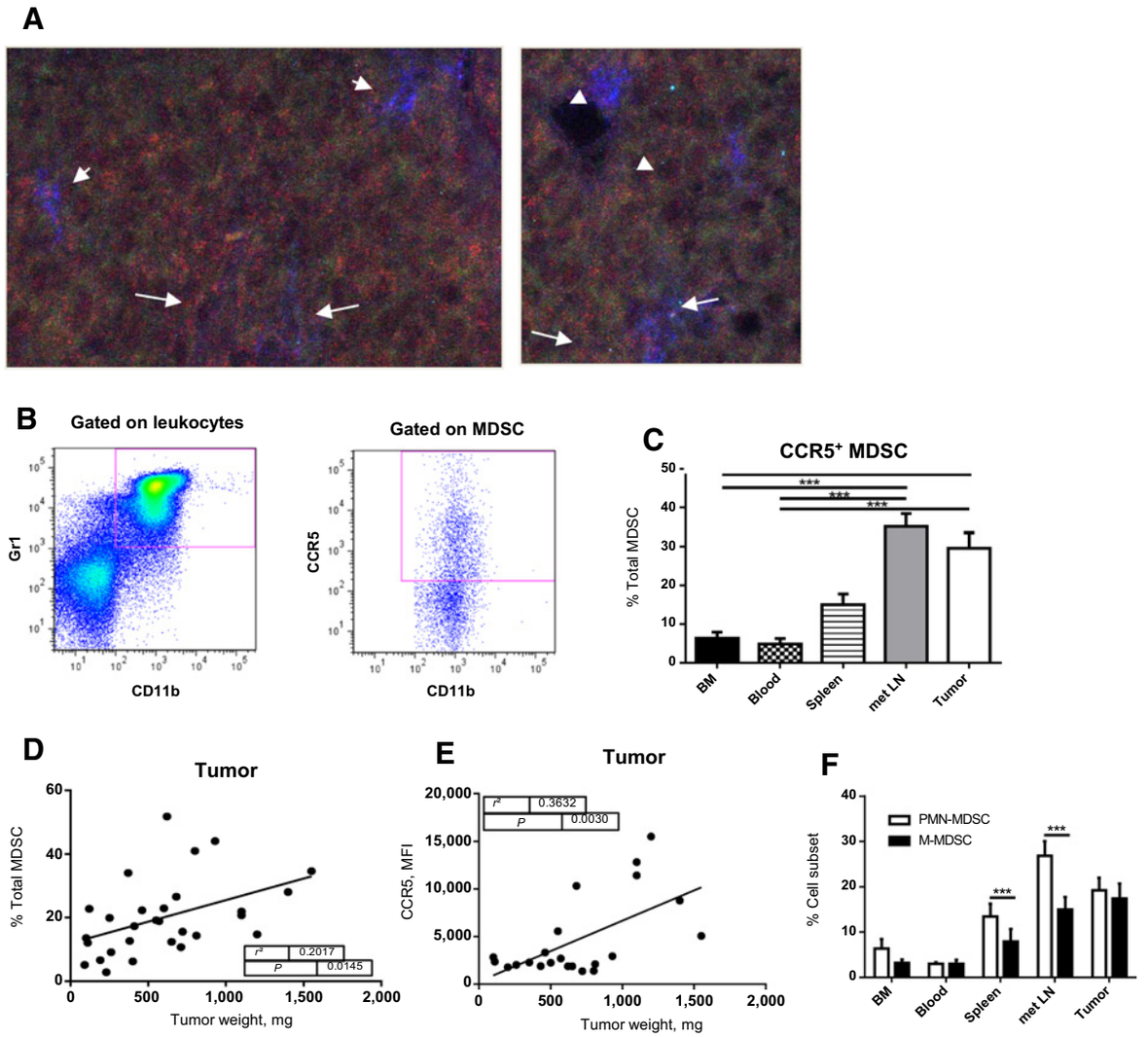

Figure 1.

Analysis of CCR5$^+$ MDSCs from tumor-bearing *Ret* transgenic mice. **A,** Immunofluorescence staining of CCR5$^+$ MDSC infiltrating skin tumors. Cells were stained for CD11b (blue), Gr1 (red), and CCR5 (green). CCR5$^+$ MDSCs are indicated with arrows, CCR5$^-$ MDSCs with arrowheads. Original magnification ×630 was used. **B,** Evaluation of CCR5 expression on MDSCs by flow cytometry. Representative dot plots for the bone marrow are shown. **C,** CCR5 expression on MDSCs was measured in the bone marrow (BM), peripheral blood, spleen, metastatic LN (met LN), skin tumors, and is presented as the percentage of CCR5$^+$ MDSC within total MDSC (mean ± SEM; $n = 23$–39 mice/group). **D** and **E,** The weight of each tumor sample was plotted against the percentage of tumor-infiltrating CCR5$^+$ MDSC within total MDSC (**D**) or the level of CCR5 expression measured as mean fluorescence intensity (MFI; **E**; $n = 29$). The correlation was calculated by linear regression analysis. **F,** CCR5 expression on M-MDSC and PMN-MDSC in the bone marrow, peripheral blood, spleen, and melanoma lesions was presented as the frequency of CCR5$^+$ cells within the respective MDSC subset. ***, $P < 0.001$.

exerted significantly stronger inhibition of T-cell proliferation than their CCR5$^-$ counterparts (Fig. 2E and F). This suggests that CCR5$^+$ subset of tumor-infiltrating MDSCs displays higher immunosuppressive potential *in vivo*.

Inflammatory factors induce the expression of CCR5 on CD11b$^+$Gr1$^+$ cells *in vitro*

To investigate the mechanism of CCR5 induction, we analyzed the effect of inflammatory factors known to stimulate MDSC recruitment (1–4, 10). CD11b$^+$Gr1$^+$ IMC were isolated from the bone marrow of C57BL/6 mice and incubated with different inflammatory mediators. We found that IL6 induced a significant upregulation of CCR5 expression on bone marrow–derived CD11b$^+$Gr1$^+$ IMC as compared with cells incubated without cytokine (Supplementary Fig. S3A; $P < 0.001$). A synergistic effect was observed when stimulating IMC with IL6 and GM-CSF. Furthermore, the combination of IL6 and GM-CSF with other factors like IL10 (Mix 1) or CCR5 ligands (Mix 2) or with CCR5 ligands, IL10, IFNγ, and IL1β (Mix 3) failed to induce an additional stimulation of CCR5 expression (Supplementary Fig. S3A). Interestingly, augmented levels of IL6 were detected within larger skin melanoma lesions (Supplementary Fig. S3B; $P < 0.002$) that

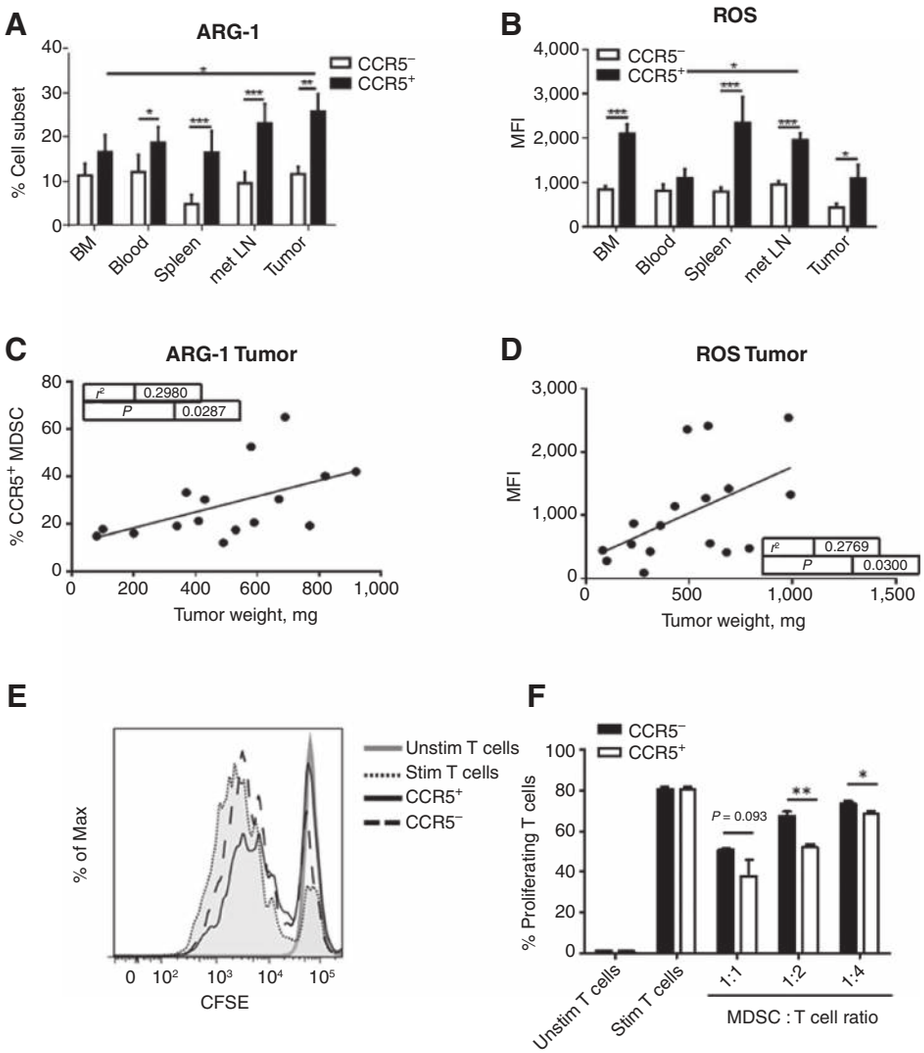

Figure 2.
Increased immunosuppressive function of CCR5$^+$ MDSCs from tumor-bearing mice. ARG-1 expression and ROS production were analyzed by flow cytometry. **A,** The frequency ARG-1–expressing cells is shown as the percentage among CCR5$^+$ or CCR5$^-$ MDSCs ($n = 18$–24 mice/group). **B,** The level of ROS production is presented as mean fluorescence intensity (MFI) ± SEM ($n = 8$–13 mice/group). The frequency of ARG-1$^+$CCR5$^+$ MDSCs (**C**; $n = 16$) or ROS levels in CCR5$^+$ MDSCs (**D**; $n = 17$) are plotted against the tumor weight. The correlation was evaluated by a linear regression analysis. **E** and **F,** CCR5$^+$ and CCR5$^-$ MDSCs were isolated from mouse tumors, followed by the coculture with normal spleen CD8$^+$ T cells labeled with CFSE and stimulated with anti-CD3/CD28 Dynabeads. **E,** A representative histogram for the inhibition of T cell proliferation by CCR5$^+$ vs. CCR5$^-$ MDSCs (MDSC:T-cell ratio=1:2). **F,** Cumulative data from one experiment out of two with similar results (mean ± SEM; $n = 6$ mice/experiment) for the inhibition of T-cell proliferation by MDSC subsets are presented as the percentage of divided T cells. MDSC:T-cell ratios were as indicated. *, $P < 0.05$; **, $P < 0.01$; ***, $P < 0.001$.

were also characterized by increased frequency of CCR5$^+$ MDSCs. Analyzing the immunosuppressive pattern of IMC treated with these inflammatory factors *in vitro*, we detected an upregulation of ARG-1 and PD-L1 expression on CCR5$^+$ cells (Supplementary Fig. S3C and S3D).

CCR5–Ig fusion protein inhibits melanoma progression and reduces tumor MDSCs *in vivo*

We next asked whether blocking CCR5/CCR5 ligand interactions could alter melanoma development. To this end, tumor-bearing transgenic mice were injected with the mCCR5–Ig fusion protein that can neutralize all three CCR5 ligands (27). Another group was treated with non-related anti-mouse IgG (control). As shown in Fig. 3A, chronic administration of mCCR5–Ig resulted in the prolongation of mouse survival as compared to the control group ($P < 0.001$). Three out of 12 mice remained alive up to 100 days upon the treatment onset. Such antitumor effect was associated with a significant decrease in the frequency of MDSCs, infiltrating primary tumors, as compared with the control group (Fig. 3B; $P < 0.05$). Importantly, tumor MDSCs from the therapy group displayed reduced immunosuppressive pattern reflected by a significantly lower NO production (Fig. 3C; $P < 0.05$). Moreover, the frequency of CCR5$^+$ MDSC infiltrating skin tumors was strongly reduced upon treatment (Fig. 3D; $P < 0.05$). Using CCR5 knockout mice, we found that the growth of transplanted Ret melanoma cells (derived from the skin tumors of *Ret* transgenic mice) was significantly reduced that was associated with a dramatic decrease in the frequency of tumor-infiltrating MDSCs (data not shown).

Because CCR5 is expressed also on T cells, including immunosuppressive regulatory T cells (Treg; ref. 29), we investigated tumor-infiltrating T lymphocytes at the same time point as MDSCs. In the control group, the frequency of CCR5$^+$ cells within CD4$^+$CD25$^+$FoxP3$^+$ Treg was significantly higher than among CD4$^+$FoxP3$^-$ conventional T cells (Tcon) and CD8$^+$ T cells (Fig. 3B; $P < 0.01$). After the therapy with mCCR5–Ig, the frequency of CCR5$^+$ Treg in primary tumors decreased as compared with the control group (Fig. 3B; $P < 0.05$). In contrast, frequencies of CD4$^+$ Tcon and CD8$^+$ T cells showed no alteration, indicating that mCCR5–Ig reduced the trafficking of MDSCs and Treg without affecting the migration of effector T cells to the tumor site.

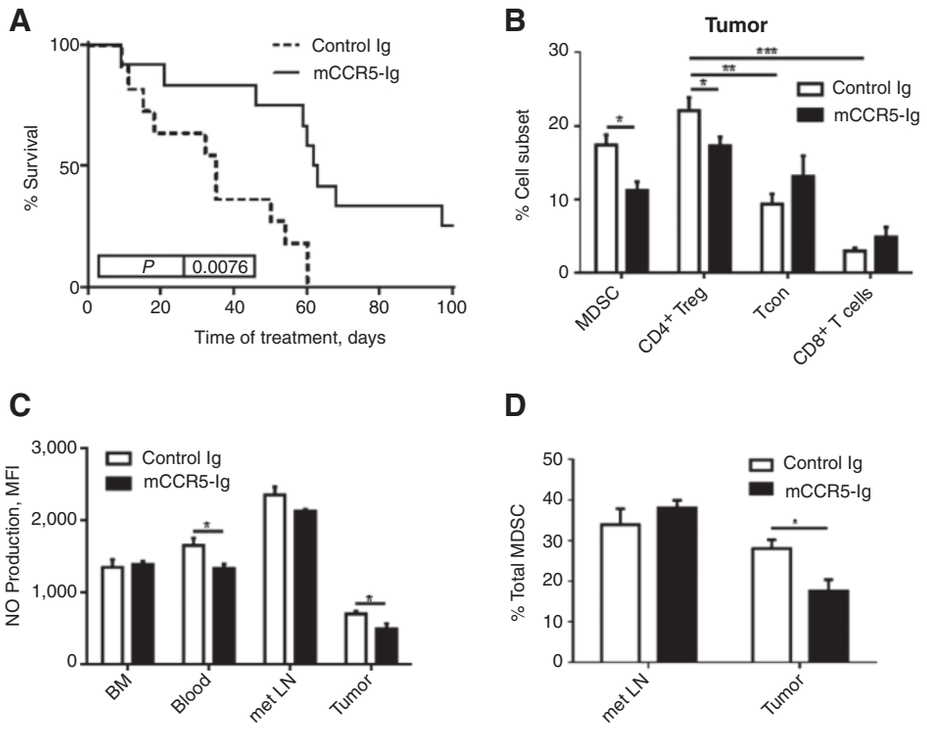

Figure 3.
Effect of mCCR5–Ig on melanoma progression. Tumor-bearing mice were injected intraperitoneally with mCCR5–Ig (10 mg/kg) twice/week for 4 weeks. Mice of control group received the same concentration of anti-mouse IgG. **A,** Mouse survival (12 mice/group) is shown as a Kaplan–Meier curve. **B,** One day after the last injection, cells from the bone marrow (BM), peripheral blood, met LN, and skin tumors were measured by flow cytometry. MDSCs are presented as the percentage of $CD45^+$ leukocytes, Tregs and Tcon as the percentage within total $CD4^+$ cells, and $CD8^+$ T cells as the percentage among total $CD3^+$ T cells (mean ± SEM; 7-8 mice/group). **C,** The level of NO production by MDSCs is shown as MFI ± SEM (7–8 mice/group). **D,** The frequency of $CCR5^+$ MDSCs in skin tumors and metastatic LN is expressed as the percentage within total MDSCs. *, $P < 0.05$; **, $P < 0.01$; ***, $P < 0.001$.

Expansion of $CCR5^+$ MDSCs in melanoma patients

Next, we analyzed the expression of CCR5 on human $HLA\text{-}DR^{-/low}CD11b^+CD14^+CD15^-$ M-MDSCs and $HLA\text{-}DR^{-/low}CD11b^+CD14^-CD15^+$ PMN-MDSCs using flow cytometry (Fig. 4A). The frequency of $CCR5^+$ M-MDSCs in the peripheral blood of melanoma patients with earlier (I and II) and advance stages (III and IV) was significantly increased as compared to their counterparts in age-matched HDs (Fig. 4B; $P < 0.01$). An elevation of $CCR5^+$ cell frequencies was demonstrated also within circulating PMN-MDSCs from these patients (Fig. 4C; $P < 0.01$). Similar to the findings in melanoma-bearing mice, the frequency of $CCR5^+$ M-MDSCs in patients' tumor samples was significantly higher than in the peripheral blood (Fig. 4D; $P < 0.05$). In contrast, we failed to observe such differences between tumor-infiltrating and circulating $CCR5^+$ PMN-MDSCs (Fig. 4E). Interestingly, the frequency of $CCR5^+$ MDSCs in melanoma patients was much higher than in tumor-bearing mice.

Enrichment of CCR5 ligands and other inflammatory factors in patients' tumor samples

To clarify the mechanisms of $CCR5^+$ MDSC enrichment in melanoma lesions, we measured inflammatory factors in serum and tumor lysates. Significantly increased levels of CCL3, CCL4 and CCL5 were detected in tumor tissue as compared with serum from the same melanoma patients (Fig. 5A–C; $P < 0.001$). Importantly, tumor lysates contained also higher concentrations of GM-CSF and IFNγ (Fig. 5D and E; $P < 0.001$). These factors induced in our *in vitro* experiments the CCR5 expression on mouse IMC (Supplementary Fig. S3A). Therefore, an enrichment of such inflammatory mediators could be responsible for the migration of $CCR5^+$ MDSCs from the peripheral blood to the tumor microenvironment.

Enhanced immunosuppressive pattern of circulating $CCR5^+$ MDSCs in melanoma patients

Next, we investigated the immunosuppressive potential of circulating $CCR5^+$ MDSCs in melanoma patients by measuring ARG-1, ROS, PD-L1, and NO in these cells. Stage III and IV patients showed elevated frequencies of $ARG\text{-}1^+CCR5^+$ M-MDSCs and $ARG\text{-}1^+CCR5^+$ PMN-MDSCs as compared with patients of earlier stages (I+II) and to their counterparts from age-matched HDs (Fig. 6A and B; $P < 0.05$). Similar results were obtained when studying the expression of PD-L1 (Supplementary Fig. S4A and S4B; $P < 0.05$) as well as the production of ROS (Supplementary Fig. S4C and S4D; $P < 0.05$) in circulating $CCR5^+$ M-MDSCs and $CCR5^+$ PMN-MDSCs from the same melanoma patients and HDs. Comparing the frequency of $ARG\text{-}1^+$ cells within circulating $CCR5^+$ and $CCR5^-$M- or PMN-MDSCs, we observed a significant increase of this parameter in $CCR5^+$ cells from patients of stage II, III, or IV (Fig. 6C and D; $P < 0.05$). Furthermore, these cells displayed stronger ARG-1 expression (Supplementary Fig. S5A and S5B; $P < 0.05$) as well as higher levels of ROS (Supplementary Fig. S5C and S5D; $P < 0.05$) as compared with $CCR5^-$ cells.

Taken together, we demonstrated that similar to tumor-bearing transgenic mice, $CCR5^+$ MDSCs are accumulated in tumor lesions of melanoma patients and displayed stronger immunosuppressive potential than $CCR5^-$ MDSCs.

Discussion

Numerous publications reported the generation, accumulation, and activation of MDSCs in mouse tumor models and cancer patients (1–4, 6–9). Because of their capacity to inhibit antitumor immune reactions mediated by T and NK cells through diverse mechanisms, MDSCs are considered as central

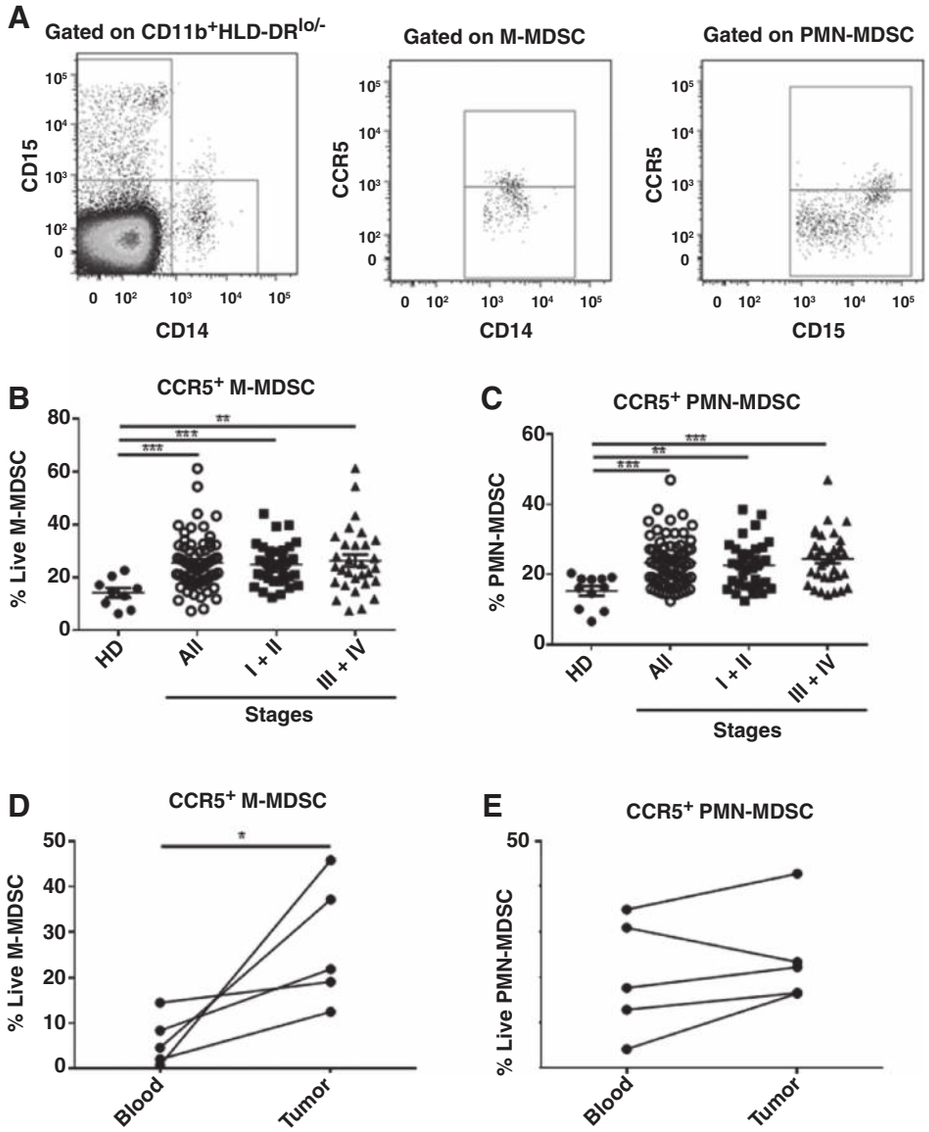

Figure 4.
CCR5 expression on MDSCs from melanoma patients. PBMCs from the peripheral blood of 66 melanoma patients of different stages and aged-matched 14 HDs were assessed by flow cytometry. **A,** Representative dot plots identifying CCR5$^+$ M-MDSCs and PMN-MDSCs. The frequency of CCR5$^+$ M-MDSCs (**B**) and CCR5$^+$ PMN-MDSCs (**C**) in melanoma patients and HDs is presented as the percentage within the total M-MDSCs or PMN-MDSCs, respectively. **D** and **E,** MDSCs from melanoma lesions and the peripheral blood of the same stage IV patients ($n = 5$) were analyzed by flow cytometry. CCR5$^+$ M-MDSCs (**D**) and PMN-MDSCs (**E**) are shown as the percentage within PBMC or leukocytes, respectively (mean ± SEM). *, $P < 0.05$; **, $P < 0.01$; ***, $P < 0.001$.

mediators of immunosuppression within the tumor microenvironment (1–3, 9–11). Several inflammatory factors were described to induce MDSCs expansion and migration, including VEGF, GM-CSF, IL6 CCL2, S100A8, and S100A9 (1–3, 7–11). However, the exact mechanisms mediating the recruitment of these cells to melanoma microenvironment are not completely clear.

The chemokine CCL5 was described to be involved in the tumor growth, invasion, angiogenesis, and immune cell recruitment to the tumor microenvironment via the interaction with its receptor CCR5 (30). Therefore, the question arises whether MDSCs could be recruited to melanoma microenvironment through CCR5/CCR5 ligand interactions. To address this question in more clinically relevant conditions, we used a *Ret* transgenic mouse melanoma model, which resembles human melanoma with respect to clinical development ensuring natural tumor–stroma interactions (25, 26). We found an increased frequency of CCR5$^+$ MDSCs in primary skin tumors and metastatic LN as compared with the bone marrow and peripheral blood. Furthermore, this accumulation was associated with melanoma progression. Interestingly, a recent study on breast cancer cells also described that CCR5$^+$ cells displayed an increased invasion and migration capacity, promoting metastasis (31).

Deciphering the mechanisms of MDSC trafficking, we demonstrated that the concentration of CCR5 ligands CCL3, CCL4, and CCL5 was significantly increased in lysates of primary tumors and metastatic LN compared with serum. These data are in agreement with publications reported that melanoma and other tumors produced elevated amounts of CCR5 ligands (9, 32–34). Interestingly, CCR5 ligands produced by melanoma-infiltrating MDSCs have been reported to attract CCR5-expressing Treg *in vitro* and *in vivo* (29). Moreover, these chemokines not only induced trafficking of CCR5$^+$ cells but also upregulated the CCR5 expression on their surface (35). In our *in vitro* experiments, CCR5 ligands enhanced the migration of CD11b$^+$Gr1$^+$ myeloid cells in the Transwell assay that could explain an accumulation of CCR5$^+$ MDSCs in melanoma lesions.

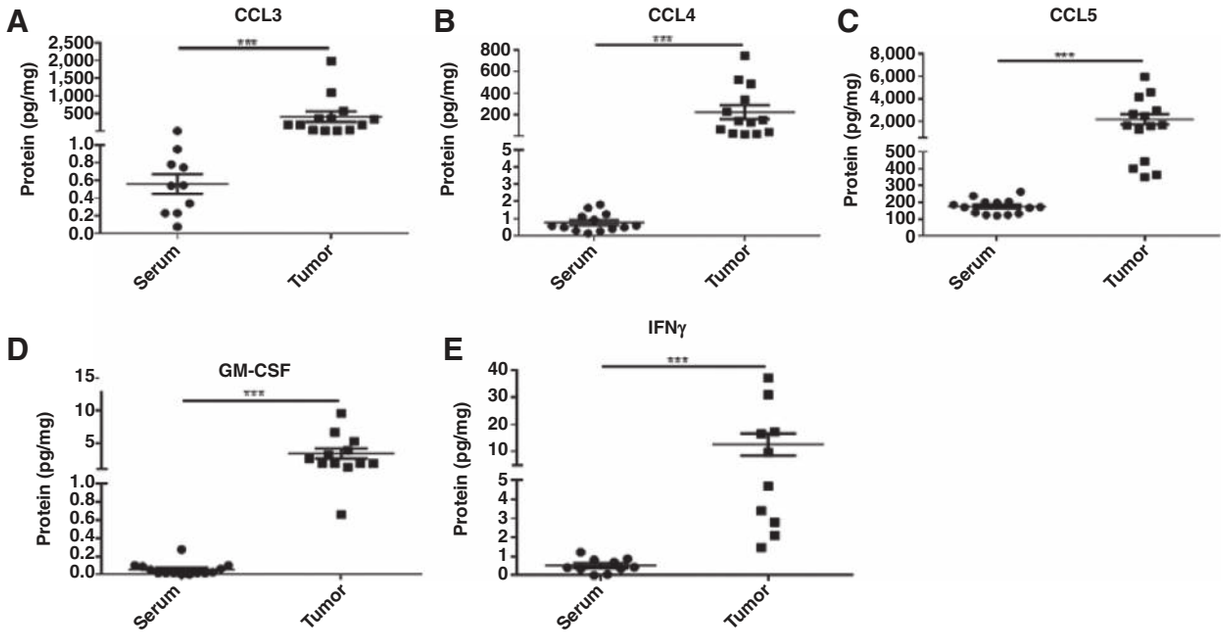

Figure 5.
Accumulation of inflammatory factors in melanoma lesions. Concentrations of CCL3 (**A**), CCL4 (**B**), CCL5 (**C**), GM-CSF (**D**), and IFNγ (**E**) were detected in serum and tumor lysates from advanced melanoma patients by Bio-Plex analysis and expressed as pg/mg protein (mean ± SEM; $n = 14$). ***, $P < 0.001$.

We have previously demonstrated that melanoma lesions from *Ret* transgenic mice contained also increasing amounts of inflammatory factors (including IL6, GM-CSF, VEGF, IL1β, IFNγ) that was associated with MDSC accumulation and fast tumor progression (36, 37). To address their potential effects on CCR5 expression, we incubated bone marrow–derived IMC with some of these factors alone or in combination with CCR5 ligands and noticed a strong increase in CCR5 expression. This

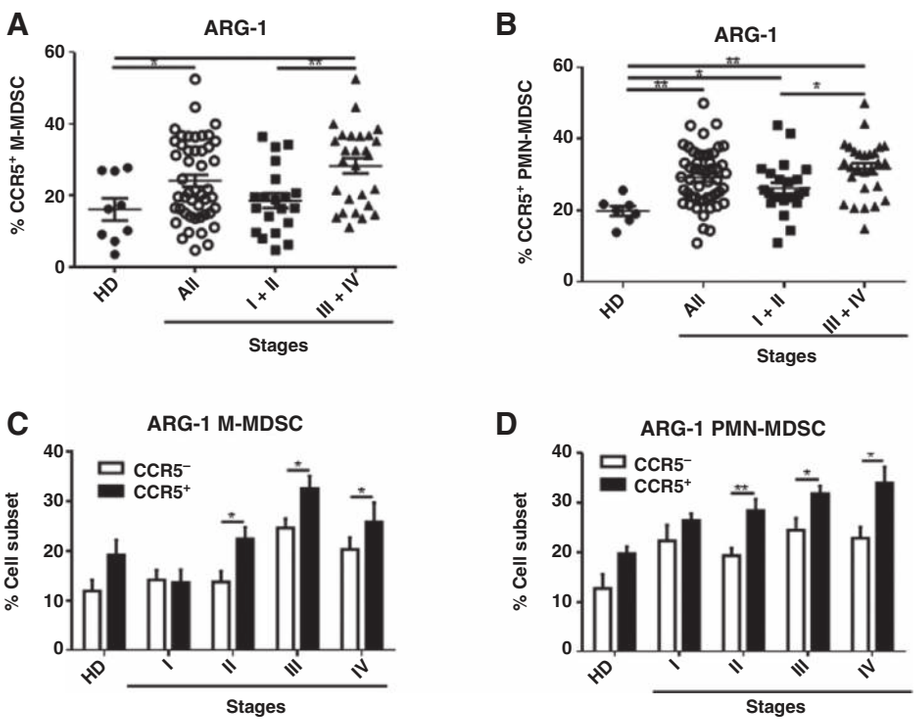

Figure 6.
Expression of ARG-1 in CCR5$^+$ MDSCs from melanoma patients. ARG-1 expression was analyzed in MDSC subsets from the peripheral blood of melanoma patients and HDs by flow cytometry. Frequencies of ARG-1$^+$ cells are presented as the percentage within CCR5$^+$ M-MDSCs (**A**) and CCR5$^+$ PMN-MDSCs (**B**). ARG-1 expression in CCR5$^+$ and CCR5$^-$ M-MDSCs (**C**) and PMN-MDSCs (**D**) is shown as the percentage of ARG-1$^+$ cells within respective subsets (mean ± SEM). *, $P < 0.05$; **, $P < 0.01$.

suggests that not only CCR5 ligands but also other inflammatory factors could mediate CCR5 upregulation on MDSCs. Other groups presented similar observation on CCR5 upregulation induced by tumor-derived colony-stimulating factor and hypoxia-inducible factor-1 in breast cancer (38, 39).

Next, we compared the immunosuppressive pattern of CCR5$^+$ and CCR5$^-$ MDSC subsets in tumor-bearing mice. We found that CCR5$^+$ MDSCs expressed significantly stronger ARG-1, ROS, PD-L1, and NO that are known to mediate MDSC function (1, 5) than their CCR5$^-$ counterparts. Importantly, this difference was especially high between MDSC subpopulations infiltrating skin tumors and metastatic LN. Moreover, an increasing production of all four immunosuppressive molecules by tumor infiltrating CCR5$^+$ MDSCs (in contrast to the CCR5$^-$ subset) significantly correlated with melanoma progression. In addition, *in vitro* incubation of bone marrow–derived CD11b$^+$Gr1$^+$ IMC with factors enriched in the tumor microenvironment (like IL6, GM-CSF, IL1β, IFNγ, IL10, and CCR5 ligands) resulted in a significant increase in PD-L1 and ARG-1 expression in CCR5$^+$ MDSCs, indicating that CCR5 ligands and other inflammatory factors could not only be involved in the migration but also in the activation of this MDSC subset. When testing CCR5 impact on MDSC immunosuppressive function, we observed that CCR5$^+$ MDSCs isolated from the skin tumors exerted significantly stronger inhibition of CD8$^+$ T-cell proliferation than their CCR5$^-$ counterparts from the same tumor lesions, suggesting an increased immunosuppressive capacity of CCR5$^+$ MDSCs. A possibility for the involvement of CCR5$^+$ Treg in the observed inhibitory effect is very low since only CD8$^+$ T cells were applied in this functional assay.

Therefore, we demonstrated for the first time that CCR5$^+$ MDSCs could not only accumulate in melanoma lesions but also display an enhanced immunosuppressive capacity. Recently, it was reported that CCR5^{high} Treg showed higher immunosuppressive activity than their CCR5^{low} Treg counterparts (40). In addition, the blockade of CCR5 signaling impaired *in vivo* suppression ability of Treg in mouse colon carcinoma model (41). However, the exact molecular mechanism of stronger immunosuppression mediated by CCR5$^+$ MDSCs was not described and is currently under investigation.

Given a critical importance of CCR5 for cell migration and activation, this receptor and its ligands were considered as therapeutic targets. It was reported that maraviroc, which binds to CCR5, mediated cytotoxic and apoptotic effects in colorectal cancer cells (42), reduced gastric cancer cell dissemination (43), and inhibited metastasis of prostate and breast cancer cells (31, 44). Furthermore, CCR5 targeting induced the repolarization of tumor-associated macrophages in colorectal cancer patients (21) and inhibited MDSC activity in the B16 melanoma mouse model (45). Targeting of CCL5 was reported to reduce MDSC functions in mammary carcinoma, leading to the inhibition of tumor progression (39).

In our experiments in transgenic melanoma-bearing mice, we applied a soluble receptor-based fusion protein mCCR5–Ig that can selectively bind and neutralize all three CCR5 ligands (CCL3, CCL4, and CCL5) simultaneously (27). We demonstrated that mice treated with mCCR5–Ig displayed a significantly prolonged survival as compared with animals injected with non-related anti-mouse IgG. Moreover, 25% of mice remained alive after 100 days of the treatment. Importantly, systemic mCCR5–Ig injections resulted in a reduced frequency of total MDSC population and CCR5$^+$ MDSC subset infiltrating skin tumors. In addition, tumor MDSCs from the therapy group displayed lower immunosuppressive pattern. Furthermore, in CCR5-deficient mice, the growth of Ret melanoma cells was significantly inhibited, which was associated with a decreased frequency of tumor-infiltrated MDSCs. These data indicate a crucial role of CCR5/CCR5 ligand interactions in the MDSC migration to the tumor site leading to the tumor progression. We observed also an inhibitory effect of mCCR5–Ig on the recruitment of Treg known to express CCR5 (29, 40, 41). In contrast, an accumulation of CD4$^+$ Tcon and CD8$^+$ T cells in melanoma lesions was not changed. This suggests that effector T cells could use other chemokine receptors for their trafficking to the tumor microenvironment and were not negatively influenced by blocking CCR5/CCR5 ligand interactions.

Next, we addressed the question on the role of CCR5$^+$ MDSCs also in melanoma patients. Analyzing M- and PMN-MDSCs subsets in the peripheral blood, we observed a significant elevation of the frequency of CCR5$^+$ cells as compared with their counterparts in age- and gender-matched HDs. Interestingly, such increase was observed already in stage I–II patients. Although an accumulation of both circulating MDSC subsets was previously described in tumor patients, including melanoma (6–8, 46–49), we demonstrated for the first time that melanoma patients displayed also increased frequency of CCR5$^+$ MDSCs. Moreover, comparing peripheral blood and tumor samples from the same patients, we found increased CCR5$^+$ M-MDSC frequencies in tumor tissues. Interestingly, we failed to observe any differences for CCR5$^+$ PMN-MDSCs. These results might be explained by a poor survival of PMN-MDSCs in our cryopreserved PBMC samples after their thawing. Similar to observations in tumor-bearing mice, we demonstrated increased concentration of CCR5 ligands in melanoma as compared with serum samples from the same patients. In addition, the level of inflammatory factors GM-CSF and IFNγ as well as IL1β (46) was elevated in melanoma microenvironment that according to our mouse data could create conditions for the MDSC migration. Analyzing the immunosuppressive pattern of MDSC subsets revealed higher expression of immunosuppressive molecules (such as ROS, ARG-1, PD-L1, and NO) in circulating CCR5$^+$ M-MDSCs and CCR5$^+$ PMN-MDSCs than in their CCR5$^-$ counterparts.

Taken together, our data highlight a key role of CCR5/CCR5 ligand interactions not only for CCR5 upregulation and driving MDSCs into melanoma microenvironment but also for their activation. Using transgenic mouse melanoma model and human melanoma samples, we demonstrated that melanoma lesions were enriched with CCR5$^+$ MDSCs showing also enhanced immunosuppressive phenotype and function as compared with CCR5$^-$ cells. Importantly, the upregulation of CCR5 expression could be achieved not only by CCR5 ligands but also by other inflammatory factors accumulated in the tumor microenvironment. The application of mCCR5–Ig reduced MDSC migration and immunosuppressive activity, leading to a significant prolongation of the survival of melanoma-bearing mice. We suggest that blocking CCR5/CCR5 ligand interactions could be applied in combined melanoma immunotherapy to neutralize MDSC-mediated immunosuppression.

Disclosure of Potential Conflicts of Interest

C. Gebhardt has received speakers bureau honoraria from BMS, MSD, Novartis, Roche, Pierre-Fabre and is a consultant/advisory board member for BMS, MSD, Novartis, Pierre-Fabre, Roche. J. Utikal has received speakers bureau honoraria from Amgen, BMS, MSD, Novartis, Roche and is a consultant/advisory Board member for Amgen, BMS, MSD, Novartis, and Roche. No potential conflicts of interest were disclosed by the other authors.

Authors' Contributions

Conception and design: C. Blattner, P. Altevogt, E. Hawila, N. Karin, V. Umansky

Development of methodology: C. Blattner, V. Fleming, R. Weber, B. Himmelhan, P. Altevogt, T.J. Schulze, H. Razon, E. Hawila, N. Karin, V. Umansky

Acquisition of data (provided animals, acquired and managed patients, provided facilities, etc.): C. Blattner, V. Fleming, R. Weber, B. Himmelhan, C. Gebhardt, H. Razon, E. Hawila, G. Wildbaum, J. Utikal, V. Umansky

Analysis and interpretation of data (e.g., statistical analysis, biostatistics, computational analysis): C. Blattner, V. Fleming, R. Weber, B. Himmelhan, P. Altevogt, C. Gebhardt, J. Utikal, V. Umansky

Writing, review, and/or revision of the manuscript: C. Blattner, V. Fleming, R. Weber, P. Altevogt, C. Gebhardt, J. Utikal, N. Karin

Administrative, technical, or material support (i.e., reporting or organizing data, constructing databases): C. Blattner, T.J. Schulze, J. Utikal, V. Umansky

Study supervision: V. Umansky

Acknowledgments

The authors thank the staff of the Core Facility Live Cell Imaging Mannheim. We thank L. Umansky and M. Platten for assistance with chemokine measurement and S. Uhlig from FlowCore Mannheim for help with the cell sorting. This work was supported by grants from German Research Council RTG2099 (to J. Utikal and V. Umansky), GE-2152/1-2 (to C. Gebhardt), DKFZ-MOST Cooperation in Cancer Research CA157 (to V. Umansky, C. Blattner, N. Karin, and H. Razon), and German Cancer Aid 109312 (to J. Utikal). This work was kindly backed by the COST Action BM1404 Mye-EUNITER.

The costs of publication of this article were defrayed in part by the payment of page charges. This article must therefore be hereby marked *advertisement* in accordance with 18 U.S.C. Section 1734 solely to indicate this fact.

Received February 2, 2017; revised February 15, 2017; accepted October 25, 2017; published OnlineFirst October 31, 2017.

References

1. Kumar V, Patel S, Tcyganov E, Gabrilovich DI. The nature of myeloid-derived suppressor cells in the tumor microenvironment. Trends Immunol 2016;37:208–20.
2. Parker KH, Beury DW, Ostrand-Rosenberg S. Myeloid-derived suppressor cells: critical cells driving immune suppression in the tumor microenvironment. Adv Cancer Res 2015;128:95–139.
3. De Sanctis F, Solito S, Ugel S, Molon B, Bronte V, Marigo I. MDSCs in cancer: Conceiving new prognostic and therapeutic targets. Biochim Biophys Acta 2016;1865:35–48.
4. Umansky V, Sevko A. Melanoma-induced immunosuppression and its neutralization. Semin Cancer Biol 2012;22:319–26.
5. Bronte V, Brandau S, Chen SH, Colombo MP, Frey AB, Greten TF, et al. Recommendations for myeloid-derived suppressor cell nomenclature and characterization standards. Nat Commun 2016;7:12150.
6. Filipazzi P, Huber V, Rivoltini L. Phenotype, function and clinical implications of myeloid-derived suppressor cells in cancer patients. Cancer Immunol Immunother 2012;61:255–63.
7. Solito S, Marigo I, Pinton L, Damuzzo V, Mandruzzato S, Bronte V. Myeloid-derived suppressor cell heterogeneity in human cancers. Ann NY Acad Sci 2014;1319:47–65.
8. Poschke I, Kiessling R. On the armament and appearances of human myeloid-derived suppressor cells. Clin Immunol 2012;144:250–68.
9. Gabrilovich DI, Ostrand-Rosenberg S, Bronte V. Coordinated regulation of myeloid cells by tumours. Nat Rev Immunol 2012;12:253–68.
10. Kanterman J, Sade-Feldman M, Baniyash M. New insights into chronic inflammation-induced immunosuppression. Semin Cancer Biol 2012;22:307–18.
11. Ostrand-Rosenberg S, Sinha P. Myeloid-derived suppressor cells: linking inflammation and cancer. J Immunol 2009;182:4499–506.
12. Homey B, Muller A, Zlotnik A. Chemokines: agents for the immunotherapy of cancer? Nature Rev Immunol 2002;2:175–84.
13. Combadiere C, Ahuja SK, Tiffany HL, Murphy PM. Cloning and functional expression of CC CKR5, a human monocyte CC chemokine receptor selective for MIP-1(alpha), MIP-1(beta), and RANTES. J Leukoc Biol 1996;60:147–52.
14. Balistreri CR, Carruba G, Calabro M, Campisi I, Di Carlo D, Lio D, et al. CCR5 proinflammatory allele in prostate cancer risk: a pilot study in patients and centenarians from Sicily. Ann N Y Acad Sci 2009;1155:289–92.
15. Luboshits G, Shina S, Kaplan O, Engelberg S, Nass D, Lifshitz-Mercer B, et al. Elevated expression of the CC chemokine regulated on activation, normal T cell expressed and secreted (RANTES) in advanced breast carcinoma. Cancer Res 1999;59:4681–87.
16. Mrowietz U, Schwenk U, Maune S, Bartels J, Küpper M, Fichtner I, et al. The chemokine RANTES is secreted by human melanoma cells and is associated with enhanced tumour formation in nude mice. Br J Cancer 1999;79:1025–31.
17. Robinson SC, Scott KA, Wilson JL, Thompson RG, Proudfoot AE, Balkwill FR. A chemokine receptor antagonist inhibits experimental breast tumor growth. Cancer Res 2003;63:8360–65.
18. Tan MC, Goedegebuure PS, Belt BA, Flaherty B, Sankpal N, Gillanders WE, et al. Disruption of CCR5-dependent homing of regulatory T cells inhibits tumor growth in a murine model of pancreatic cancer. J Immunol 2009;182:1746–55.
19. Zhang X, Haney KM, Richardson AC, Wilson E, Gewirtz DA, Ware JL, et al. Anibamine, a natural product CCR5 antagonist, as a novel lead for the development of anti-prostate cancer agents. Bioorg Med Chem Lett 2010;20:4627–30.
20. Velasco-Velazquez M, Jiao X, De La Fuente M, Pestell TG, Ertel A, Lisanti MP, et al. CCR5 antagonist blocks metastasis of basal breast cancer cells. Cancer Res 2012;72:3839–50.
21. Halama N, Zoernig I, Berthel A, Kahlert C, Klupp F, Suarez-Carmona M, et al. Tumoral immune cell exploitation in colorectal cancer metastases can be targeted effectively by anti-CCR5 therapy in cancer patients. Cancer Cell 2016;29:587–601.
22. Lesokhin AM, Hohl TM, Kitano S, Cortez C, Hirschhorn-Cymerman D, Avogadri F, et al. Monocytic CCR2(+) myeloid-derived suppressor cells promote immune escape by limiting activated CD8 T-cell infiltration into the tumor microenvironment. Cancer Res 2012;72:876–86.
23. Izhak L, Wildbaum G, Zohar Y, Anunu R, Klapper L, Elkeles A, et al. A novel recombinant fusion protein encoding a 20-amino acid residue of the third extracellular (E3) domain of CCR2 neutralizes the biological activity of CCL2. J Immunol 2009;183:732–9.
24. Izhak L, Wildbaum G, Jung S, Stein A, Shaked Y, Karin N. Dissecting the autocrine and paracrine roles of the CCR2-CCL2 axis in tumor survival and angiogenesis. PLoS ONE 2012;7:e28305.
25. Kato M, Takahashi M, Akhand AA, Liu W, Dai Y, Shimizu S, et al. Transgenic mouse model for skin malignant melanoma. Oncogene 1998;17:1885–8.
26. Umansky V, Abschuetz O, Osen W, Ramacher M, Zhao F, Kato M, et al. Melanoma-specific memory T cells are functionally active in Ret transgenic mice without macroscopic tumors. Cancer Res 2008;68:9451–8.
27. Sapir Y, Vitenshtein A, Barsheshet Y, Zohar Y, Wildbaum G, Karin N. A fusion protein encoding the second extracellular domain of CCR5 arrests chemokine-induced cosignaling and effectively suppresses ongoing experimental autoimmune encephalomyelitis. J Immunol 2010;185:2589–99.

28. Zohar Y, Wildbaum G, Novak R, Salzman AL, Thelen M, Alon R, et al. CXCL11-dependent induction of FOXP3-negative regulatory T cells suppresses autoimmune encephalomyelitis. J Clin Invest 2014;124:2009–22.
29. Schlecker E, Stojanovic A, Eisen C, Quack C, Falk CS, Umansky V, et al. Tumor-infiltrating monocytic myeloid-derived suppressor cells mediate CCR5-dependent recruitment of regulatory T cells favoring tumor growth. J Immunol 2012;189:5602–11.
30. Appay V, Rowland-Jones SL. RANTES: a versatile and controversial chemokine. Trends Immunol 2001;22:83–7.
31. Velasco-Velazquez M, Jiao X, De La Fuente M, Pestell TG, Ertel A, Lisanti MP, et al. CCR5 antagonist blocks metastasis of basal breast cancer cells. Cancer Res 2012;72:3839–50.
32. Zhu Z, Aref AR, Cohoon TJ, Barbie TU, Imamura Y, Yang S, et al. Barbie, Inhibition of KRAS-driven tumorigenicity by interruption of an autocrine cytokine circuit. Cancer Discov 2014;4:452–65.
33. Aldinucci D, Colombatti A. The inflammatory chemokine CCL5 and cancer progression. Mediators Inflamm 2014;2014:292376.
34. Richmond A, Yang J, Su Y. The good and the bad of chemokines/chemokine receptors in melanoma. Pigment Cell Melanoma Res 2009;22: 175–86.
35. Gao D, Rahbar R, Fish EN. CCL5 activation of CCR5 regulates cell metabolism to enhance proliferation of breast cancer cells. Open Biol 2016;6:160122.
36. Meyer C, Sevko A, Ramacher M, Bazhin AV, Falk CS, Osen W, et al. Chronic inflammation promotes myeloid-derived suppressor cell activation blocking antitumor immunity in transgenic mouse melanoma model. Proc Natl Acad Sci U S A 2011;108:17111–6.
37. Sevko A, Michels T, Vrohlings M, Umansky L, Beckhove P, Kato M, et al. Antitumor effect of paclitaxel is mediated by inhibition of myeloid-derived suppressor cells and chronic inflammation in the spontaneous melanoma model. J Immunol 2013;190:2464–71.
38. Lin S, Wan S, Sun L, Hu J, Fang D, Zhao R, et al. Chemokine C-C motif receptor 5 and C-C motif ligand 5 promote cancer cell migration under hypoxia. Cancer Sci 2012;103:904–12.
39. Zhang Y, Lv D, Kim HJ, Kurt RA, Bu W, Li Y, et al. A novel role of hematopoietic CCL5 in promoting triple-negative mammary tumor progression by regulating generation of myeloid-derived suppressor cells. Cell Res 2013;23:394–408.
40. Ward ST, Li KK, Hepburn E, Weston CJ, Curbishley SM, Reynolds GM, et al. The effects of CCR5 inhibition on regulatory T-cell recruitment to colorectal cancer. Br J Cancer 2015;112:319–28.
41. Chang LY, Lin YC, Kang CW, Hsu CY, Chu YY, Huang CT, et al. The indispensable role of CCR5 for *in vivo* suppressor function of tumor-derived CD103+ effector/memory regulatory T cells. J Immunol 2012; 189:567–74.
42. Pervaiz A, Ansari S, Berger MR, Adwan H. CCR5 blockage by maraviroc induces cytotoxic and apoptotic effects in colorectal cancer cells. Med Oncol 2015;32:158.
43. Mencarelli A, Graziosi L, Renga B, Cipriani S, D'Amore C, Francisci D, et al. CCR5 antagonism by maraviroc reduces the potential for gastric cancer cell dissemination. Transl Oncol 2013;6:784–93.
44. Sicoli D, Jiao X, Ju X, Velasco-Velazquez M, Ertel A, Addya S, et al. CCR5 receptor antagonists block metastasis to bone of v-Src oncogene-transformed metastatic prostate cancer cell lines. Cancer Res 2014;74:7103–14.
45. Tang Q, Jiang J, Liu J. CCR5 blockade suppresses melanoma development through inhibition of IL-6-Stat3 pathway via upregulation of SOCS3. Inflammation 2015;38:2049–56.
46. Jiang H, Gebhardt C, Umansky L, Beckhove P, Schulze TJ, Utikal J, et al. . Elevated chronic inflammatory factors and myeloid-derived suppressor cells indicate poor prognosis in advanced melanoma patients. Int J Cancer 2015;136:2352–60.
47. Weide B, Martens A, Zelba H, Stutz C, Derhovanessian E, Di Giacomo AM, et al. Myeloid-derived suppressor cells predict survival of advanced melanoma patients: comparison with regulatory T cells and NY-ESO-1- or Melan-A-specific T cells. Clin Cancer Res 2014;20:1601–9.
48. Jordan KR, Amaria RN, Ramirez O, Callihan EB, Gao D, Borakove M, et al. Myeloid-derived suppressor cells are associated with disease progression and decreased overall survival in advanced-stage melanoma patients. Cancer Immunol Immunother 2013;62:1711–22.
49. Schilling B, Sucker A, Griewank K, Zhao F, Weide B, Görgens A, et al. Vemurafenib reverses immunosuppression by myeloid-derived suppressor cells. Int J Cancer 2013;133:1653–63.